

Method for Organizing Symmetrical Distribution of Discharge Current in a Magnetoplasma Compressor at Elevated Operating Pressures

© A.S. Pashchina

Joint Institute for High Temperatures, Russian Academy of Sciences, Moscow, Russia
E-mail: fgrach@mail.ru

Received August 14, 2025

Revised August 31, 2025

Accepted September 1, 2025

A method for organizing a discharge in a magnetoplasma compressor, ensuring an axisymmetric distribution of the discharge current, is proposed and implemented. This is made possible by dividing the external electrode into isolated segments that are connected to the output of a binary branched electrical circuit, which provides automatic adjustment of electrical parameters due to negative feedback created by a system of bifilarly coupled inductors. The proposed solution allows raising the operating pressure threshold up to atmospheric values. A criterion for selecting the parameters of bifilar inductors that ensures minimal current imbalance in the arrester sections has been obtained.

Keywords: magnetoplasma compressor, coaxial electrodes, axial symmetry, autotuning, binary branched electric circuit.

DOI: 10.61011/TPL.2026.01.62818.20472

A magnetoplasma compressor (MPC) is an electromagnetic accelerator with coaxial electrodes that produces compressive flows of the plasma focus type with extreme plasma parameters [1–3]. MPCs find application in thermonuclear fusion [1,4–6], magnetoplasma aerodynamics [7], and plasma technologies [8], are used as high-power sources of ultraviolet radiation [9], etc. In recent years, the interest in MPCs was kept up owing to the construction of high-power electric jet engines capable of operating both in a dense atmosphere and in vacuum [2,7,10,11].

Axial symmetry of the discharge current distribution is the key prerequisite for efficient plasma acceleration in coaxial arresters [1,12]. This condition is fulfilled within a limited range of operating pressures ($p = 10^{-5} - 10$ Torr) as long as a diffuse discharge form persists. The formation of electrode spots, discharge pinching, and other effects observed at pressures above $p > 100$ Torr lead to violation of the axial symmetry of the discharge and, ultimately, to acceleration mode breakdown.

It was shown in [11] that the upper threshold of operating pressures of MPCs with a symmetrical distribution of discharge current may be extended to atmospheric values by using an initiating discharge of a nanosecond duration. Another method, which was proposed in [13], involves dividing the external electrode into isolated segments and connecting each of them through a controlled switch to a separate capacitor bank of a sectioned power supply. However, the possibility of discharge symmetry violation both at the breakdown stage and within the main discharge pulse (e.g., due to uncontrolled fluctuations in parameters) still remains in both cases.

The method discussed below allows one to eliminate the mentioned disadvantages. It relies on dividing the external MPC electrode into isolated segments and establishing

negative feedback between them by means of bifilarly coupled inductors, which ensure synchronous ignition and automatic equalization of currents in the event of an imbalance. Bifilar inductors are the elements of a binary branched electric circuit (BBEC), and electrically isolated segments of the external electrode of the arrester are its end links. Both an AC voltage source and a storage capacitor connected via a controlled switch may serve as a BBEC power supply.

Figure 1 shows the structural diagram of a three-level BBEC with isolated segments of the external electrode being the closing links of the third level and provides a clear illustration of the principles of its design and operation. In the general case, the number of segments of the external electrode is set by BBEC level n and is exactly equal to the number of branches of its last level (i.e., 2^n). Each pair of magnetically coupled inductors provides negative feedback between the branches emerging from a common node. The inductors are wound on a single frame, and their electric wiring, which ensures that magnetic fluxes are directed oppositely, facilitates the equalization of currents flowing in them. Thus, one pair of inductors of upper level i helps equalize currents at the connection nodes of two pairs of inductors of lower level $(i + 1)$, and each pair of inductors of last level n helps equalize currents that close on two arrester segments. In a three-level BBEC (Fig. 1, a), this function is fulfilled by four pairs of third-level inductors (L_{31}/L_{32} , L_{33}/L_{34} , L_{35}/L_{36} , and L_{37}/L_{38}) that ensure current equalization in an eight-section arrester (here and elsewhere, the first and second subscripts of L correspond to ordinal numbers of the level and the branch, respectively).

The total number of inductors of a BBEC of level n is equal to the number of its branches: $N = \sum_{m=0}^{n-1} 2^{n-m}$. The

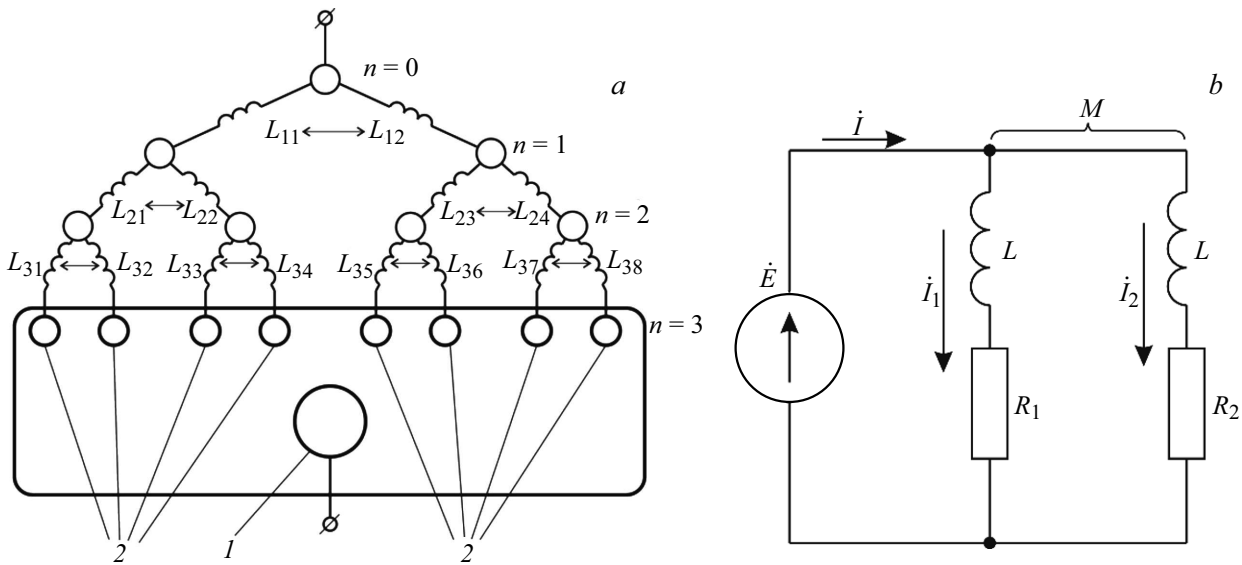


Figure 1. *a* — Structural diagram of a three-level BBEC with negative feedback formed by a system of bifilar inductors that provides automatic adjustment of the electrical parameters of adjacent branches; *b* — equivalent circuit of a single-level BBEC for estimating current imbalance and selecting inductor parameters. *I* — Central electrode; *2* — sections of the external electrode.

number of bifilarly coupled pairs is equal to the number of branching nodes (i. e., is two times lower).

When selecting the inductor parameters, we may limit ourselves to the examination of the final stage, since its parameters are the ones that govern the current imbalance in load branches (arresters). The equivalent circuit of the end stage cell (Fig. 1, *b*) may be reduced to a single-level BBEC [14]. We assume that the circuit is powered by an alternating voltage \dot{E} source (the dot above denotes complex variables) and its branches are loaded by various active resistances $R_1 > R_2$, which simulate the plasma resistance in arrester sections.

The ratio of currents in parallel branches is

$$\frac{i_1}{i_2} = \frac{R_2 + j\omega L(1+k)}{R_1 + j\omega L(1+k)}, \quad (1)$$

which yields disbalance of amplitude current values

$$\delta|i| = 1 - \frac{|i_1|}{|i_2|} = 1 - \sqrt{\frac{\left(\frac{R_2}{R_1}\right)^2 + \left(\frac{\omega L(1+k)}{R_1}\right)^2}{1 + \left(\frac{\omega L(1+k)}{R_1}\right)^2}}. \quad (2)$$

Here, $k = M/L$ is the coupling coefficient for a pair of inductors ($k \approx 1$ for bifilar winding), M is the mutual induction coefficient, and ω is the circular frequency of the power supply.

It follows from (1) and (2) that the reactive component of resistance of the branch with the highest active resistance should exceed its active component if a current imbalance is to be reduced: $\omega L(1+k) > R_1$. For example, with a tenfold difference in active resistances ($R_1/R_2 = 10$), the reactive component of resistance needs to be just 7 times

higher than the active one,

$$\frac{\omega L(1+k)}{R_1} = \sqrt{\frac{(1 - \delta|i|)^2 - \left(\frac{R_2}{R_1}\right)^2}{1 - (1 - \delta|i|)^2}} = 7, \quad (3)$$

to maintain a disbalance of amplitude current values $\delta|i| < 1\%$. Relation (3) may be regarded as a criterion for selecting the parameters of bifilar inductors based on the requirements for current imbalance in arrester sections.

The equalization of currents in parallel branches is facilitated by the EMF of mutual induction of a pair of inductors, which induces a synchronous increase and decrease in voltage at higher and lower resistances, respectively. In the above example, the ratio of amplitude voltage values is approximately equal to the ratio of active resistances:

$$\frac{|\dot{U}_1|}{|\dot{U}_2|} = 9.9 \approx \frac{R_1}{R_2}.$$

This corresponds to an almost ten-to-one power ratio at resistances R_1 and R_2 . If the load is plasma produced in arrester sections, an increase in power in one section and a decrease in the other will cause a corresponding increase and decrease in plasma ionization degree, which will ultimately lead to equalization of the electrical conductivity of plasma in these sections.

If, for example, a discharge was ignited in one section only, the flow of current in this section will lead to an increase in voltage at the electrodes of the second section. In the limit case ($R_1 = 0$, $R_2 = \infty$, $k = 1$), the amplitude of voltage at the second section

$$\frac{|\dot{U}_2|}{|\dot{E}|} = \sqrt{\frac{1 + (\omega L(1+k)/R_1)^2}{1 + (\omega L/R_1)^2}}$$

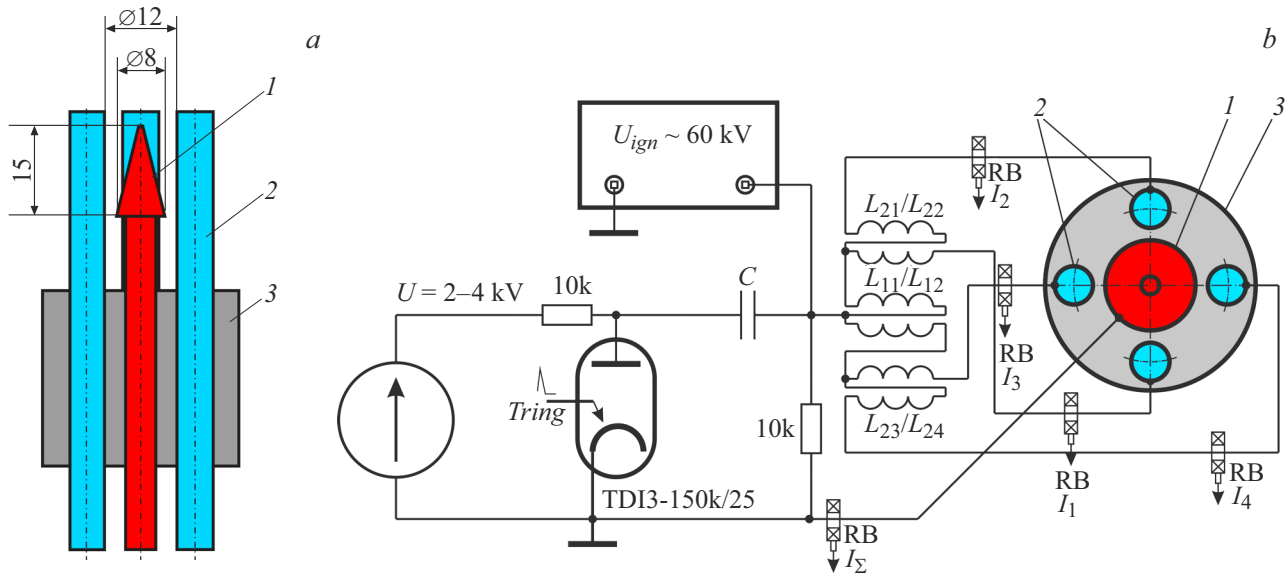


Figure 2. *a* — Structural diagram of an MPC with an external electrode made of four electrically isolated segments; *b* — schematic circuit diagram of the experimental setup based on a two-level BBEC. 1 — Central electrode, 2 — isolated segments of the external electrode, and 3 — housing.

exceeds power supply voltage \dot{E} by a factor of 2, facilitating the ignition of a discharge in this section. The current in the first section

$$\dot{I}_1 = \frac{\dot{E}}{R_1 + j\omega L}$$

is then maintained at the minimum level until the moment of discharge ignition in the second section.

Two important advantages of the proposed method should be noted. The first one is the synchronization of the processes of current rise in all arrester sections. This is especially important if breakdowns in sections are not simultaneous. A synchronous increase in current in all sections will be observed only after the ignition of a discharge in the last section. Until this moment, the current through the sections where a breakdown has already occurred will be suppressed by the counter EMF produced by bifilar inductors. The second advantage is that discharge ignition is guaranteed in all sections, since a discharge in one of them will automatically induce an increase in voltage at the remaining sections.

Experimental studies were performed for the simplest MPC modification containing a central electrode in the form of a truncated cone and four isolated sections of the external electrode (Fig. 2, *a*), which were connected to the output of a two-level BBEC (Fig. 2, *b*). Voltage from the power source (a capacitor bank with capacitance $C = 200-500 \mu\text{F}$ charged to voltage $U = 2-4 \text{ kV}$) was fed to its input. The two-level BBEC consisted of three pairs of bifilar inductors. Two of them (L_{21}/L_{22} and L_{23}/L_{24}) provided automatic adjustment of currents closing on the segments of the external MPC electrode, and one pair (L_{11}/L_{12}) ensured equalization of currents at the connection nodes of bifilar

inductors L_{21}/L_{22} and L_{23}/L_{24} (Fig. 2, *b*). The inductance of a single inductor in a bifilar pair was $L_i = 21 \mu\text{H}$, and the inductance of a pair of inductors with opposite wiring was $L_b = 0.8 \mu\text{H}$, which corresponds to coupling coefficient $k = 1 - L_b/2L = 0.98$.

Voltage was supplied to the external MPC electrodes at the moment a TDI3-150k/25SNP thyatron was actuated. A high-voltage source with a voltage amplitude up to $U_{ign} = 60 \text{ kV}$ and pulse duration $t_{ign} \sim 10 \mu\text{s}$ was used to ignite a discharge. The main discharge proceeded with a delay of $t_{del} \sim 10 \mu\text{s}$ relative to the thyatron actuation. A BNC-575 (Berkley Nucleonics Corporation, United States) delay and pulse generator was used for synchronization of the auxiliary and main discharges and the recording equipment. Total current I_Σ and currents I_1-I_4 closing on the external electrode sections were measured with a Rogowski coil (RC), which was inserted in the corresponding branch of the electrical circuit (connection points are marked in Fig. 2, *b*). A Tektronix P6015A high-voltage probe was used for voltage measurements.

Figure 3 shows high-speed video frames (side view and end view) characterizing the discharge dynamics. Experiments were carried out in air under normal conditions ($p = 760 \text{ Torr}$, $T = 293 \text{ K}$). Numerous trials revealed that a discharge is ignited simultaneously in all four sections. As the discharge current increases, all four plasma channels move synchronously along the surface of electrodes toward the arrester output section. When the threshold value of discharge current, which is 15 kA for the given arrester dimensions (Fig. 2, *a*), is exceeded, a plasma focus is formed at the output (see the frame with time stamp $t = 62.5 \mu\text{s}$ in Fig. 3).

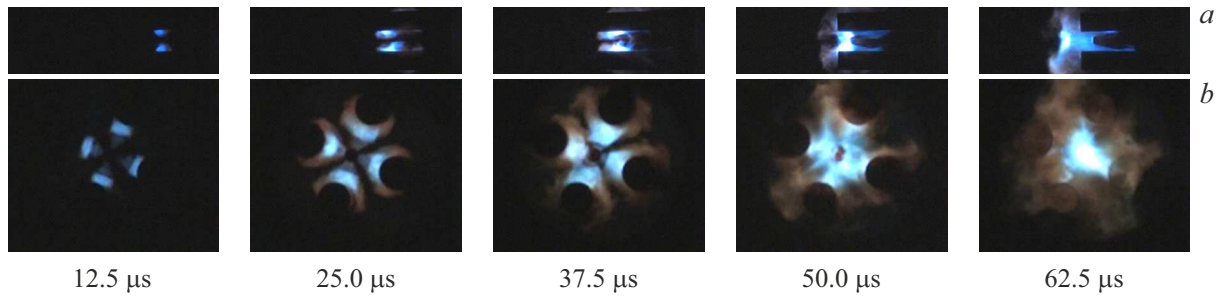


Figure 3. Dynamics of an MPC discharge in air at atmospheric pressure with an external electrode made of four electrically isolated segments. *a* — Side view; *b* — end view. Storage capacitor voltage $U_C = 4\text{ kV}$; discharge current amplitude $I_m = 30\text{ kA}$. Frames were recorded using a Phantom VEO 310 high-speed video camera with an exposure time of $1\text{ }\mu\text{s}$. Time elapsed from the moment of discharge ignition is indicated below.

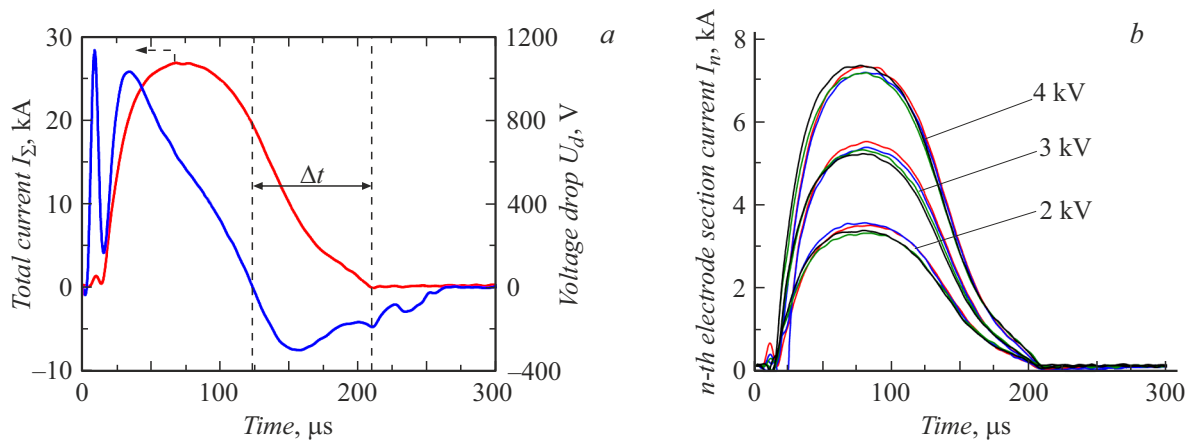


Figure 4. Oscilloscope records of total current and voltage at one of the MPC electrodes at a storage capacitor voltage of 4 kV (*a*) and oscilloscope records of current in isolated segments of the external electrode at a storage capacitor voltage of 2, 3, and 4 kV (*b*).

Figure 4, *a* shows the typical oscilloscope records of total current and voltage measured at the input of the branched circuit. At storage capacitor voltage $U = 4\text{ kV}$, the total amplitude of discharge current reaches $I_\Sigma \approx 30\text{ kA}$, and the discharge pulse duration is $\tau_d = 200\text{ }\mu\text{s}$. The presence of a phase shift between current and voltage (this is indicated by a change in voltage sign that occurs long before the moment of discharge extinction ($\Delta t \approx 70\text{ }\mu\text{s}$)) is a characteristic sign of plasma acceleration via the magnetohydrodynamic mechanism [15]. With the chosen parameters of matching inductors, the imbalance of currents and voltages at the isolated arrester segments does not exceed the experimental error ($\delta I < 10\%$), which is confirmed by the corresponding measurements performed at different storage capacitor voltages (Fig. 4, *b*).

Thus, regardless of the working gas pressure, the proposed method solves completely the problem of axial symmetry of the discharge current distribution in arresters with coaxial electrodes. The scope of application of this method is not limited to coaxial and/or multi-section arresters. It may be used, e.g., to implement synchronous ignition and automatic adjustment of parameters in a system of independent arresters, equalize currents in active loads, etc.

Funding

This study was supported financially by the Ministry of Science and Higher Education of the Russian Federation (state assignment No. 075-00269-25-00).

Conflict of interest

The author declares that he has no conflict of interest.

References

- [1] A.I. Morozov, *Fiz. Plazmy*, **16** (2), 131 (1990) (in Russian).
- [2] A.A. Kartasheva, K.M. Gutorov, V.L. Podkovyrov, E.A. Muravyeva, K.S. Lukyanov, N.S. Klimov, *Phys. Plasmas*, **31** (4), 043107 (2024). DOI: 10.1063/5.0198341
- [3] I.E. Garkusha, D.G. Solyakov, V.V. Chebotarev, V.A. Makhlay, N.V. Kulik, *Plasma Phys. Rep.*, **45** (2), 166 (2019). DOI: 10.1134/S1063780X19010057.
- [4] U. Shumlak, *J. Appl. Phys.*, **127** (20), 200901 (2020). DOI: 10.1063/5.0004228
- [5] E.J. Lerner, S.M. Hassan, I. Karamitsos, F. Von Roessel, *Phys. Plasmas*, **24** (10), 102708 (2017). DOI: 10.1063/1.4989859
- [6] S. Singha, P.P. Kalita, A. Ahmed, P. Baruah, B. Bhattacharya, N.K. Neog, T.K. Borthakur, *Phys. Plasmas*, **32** (8), 083101 (2025). DOI: 10.1063/5.0272376

- [7] I.C. Mashek, V.A. Lashkov, Y.F. Kolesnichenko, V.G. Brovkin, in *49th AIAA Aerospace Sciences Meeting including the New Horizons Forum and Aerospace Exposition* (Orlando, Florida, 2011), p. 1–6. DOI: 10.2514/6.2011-1274
- [8] S. Auluck, P. Kubes, M. Paduch, M.J. Sadowski, V.I. Krauz, S. Lee, L. Soto, M. Scholz, R. Miklaszewski, H. Schmidt, A. Blagoev, M. Samuelli, Y.S. Seng, S.V. Springham, A. Talebitaher, C. Pavez, M. Akel, S.L. Yap, R. Verma, K. Kollacek, P.L.C. Keat, R.S. Rawat, A. Abdou, G. Zhang, T. Laas, *Plasma*, **4** (3), 450 (2021). DOI: 10.3390/plasma4030033
- [9] V.V. Kuzenov, A.Y. Varaksin, S.V. Ryzhkov, *Symmetry*, **16** (9), 1200 (2024). DOI: 10.3390/sym16091200
- [10] R.L. Burton, D.L. Carroll, J.W. Zimmerman, US patent 2023/0413414 A1 (2023).
- [11] B. Göksel, I.C. Mashek, *J. Phys.: Conf. Ser.*, **825**, 012005 (2017). DOI: 10.1088/1742-6596/825/1/012005
- [12] A.K. Vinogradova, A.I. Morozov, in *Fizika i primeneniye plazmennykh uskoritelei*, Ed. by A.I. Morozov (Nauka Tekh., Minsk, 1974), p. 103 (in Russian).
- [13] L.Ya. Min'ko, V.M. Astashinskii, *Ustroistvo tortsevogo tipa dlya polucheniya plazmennykh strui*, Author's Certificate No. 915772. *Byull. Izobret.* No. 30 (October 15, 1982) (in Russian).
- [14] K.M. Polivanov, *Teoreticheskie osnovy elektrotehniki* (Energiya, M.–L., 1965), Vol. 1 (in Russian).
- [15] J. Puric, I.P. Dojcinovic, V.M. Astashynski, M.M. Kuraica, B.M. Obradovic, *Plasma Sources Sci. Technol.*, **13** (1), 74 (2004). DOI: 10.1088/0963-0252/13/1/010

Translated by D.Safin